



INFINITE TRANSITION-ENERGY LATTICE  
USING  $\pi$ -STRAIGHT SECTIONS

L. C. Teng

July 16, 1971

It is generally known that with reverse bending one can push  $\gamma_t$  (transition  $\gamma$ ) to  $\infty$  in a lattice (V.V. Vladimirski and E.K. Tarasov, "Theoretical Problems of the Ring Accelerators," Moscow, Academy of Sciences, 1955). We want to show here that the same can be accomplished by judicious insertion of the  $\pi$ -straight sections (A.A. Garren, p. 22, Proceedings of the V International Conference on High Energy Accelerators, Frascati, 1965). This effect was noticed, for example, in the lattice of the 500 MeV booster proposed for the Argonne ZGS (Argonne National Laboratory Accelerator Division Proposal, June 1969).



# I. GEOMETRICAL OBSERVATION

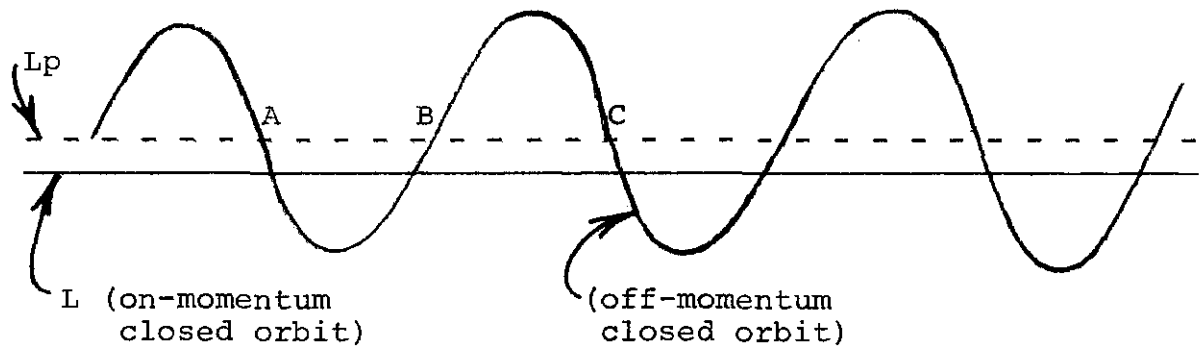


Figure 1

In an AG lattice if the on-momentum closed orbit is shown stretched out as straight line L (Fig. 1), the off-momentum orbit is oscillatory about line L. Because of the curvature of L (say, downward) an inward-swing section such as AB of the off-momentum orbit has a negative first-order length increment and an outward-swing section such as BC has a positive first-order length increment. The net orbit length increment is generally positive but rather small and corresponds roughly to that of the mean orbit shown as dotted straight line  $L_p$ . An AG lattice, therefore, generally has a small dispersion orbit-length increment, hence a large momentum compaction.

The concept of reducing (to zero) the dispersion orbit-length increment by introducing reverse bending is as follows: If the curvature of the on-momentum orbit L is reversed over the section BC the first-order orbit-length increment over BC will also reverse sign and become negative. The combined

orbit-length increment over AB and BC will, then, have a large excess negative value. By introducing a few such reverse bends it is possible to totally compensate the small net positive orbit-length increment corresponding to that of  $L_p$  and obtain a zero total dispersion orbit-length increment, hence  $\infty$  momentum compaction and infinite  $\gamma_t$ .

An interesting variance of this concept is the following: Instead of a reverse bend over BC one can make the orbit curvature zero, i.e., make section BC into a  $\pi$ -straight section. In this case the first-order orbit-length increment over BC is zero and the combined increment over AB and BC still has a large excess negative value although it is only roughly half that of the case with the reverse bend. Zero total dispersion orbit-length increment and infinite  $\gamma_t$  can similarly be attained. Compared to the case with reverse bending the  $\pi$ -insertion lattice has the following practical advantages:

- (a) No reverse bending magnet is required.
- (b) Long straight sections in a lattice are needed anyway for injection, extraction, rf cavities, etc.

It is clear from the discussion that any matched long straight section with a large phase advance close to  $\pi$  can be used effectively over section BC. But  $\pi$ -straight section is the simplest and can be analyzed most easily.

## II. DISPERSION FORMALISM

We will write the 3 x 3 horizontal optics-dispersion transfer matrix as

$$\begin{pmatrix} a & b & e \\ c & d & f \\ 0 & 0 & 1 \end{pmatrix} \equiv (M|D) \quad (1)$$

where

$$\begin{cases} M = \begin{pmatrix} a & b \\ c & d \end{pmatrix} = 2 \times 2 \text{ optics transfer matrix} \\ D = \begin{pmatrix} e \\ f \end{pmatrix} = \text{dispersion transfer vector.} \end{cases}$$

The following rules of multiplication are obvious:

(a) If a dispersion vector  $\begin{pmatrix} \xi \\ \xi' \\ 1 \end{pmatrix}$  is written as

$$\Xi = \begin{pmatrix} \xi \\ \xi' \end{pmatrix}$$

then

$$(M|D)\Xi = M\Xi + D. \quad (2)$$

$$(b) \quad (M_2|D_2)(M_1|D_1) = (M_2M_1|M_2D_1+D_2) \quad (3)$$

$$(c) \quad (M|D)^n = (M^n|(1-M^n)(1-M)^{-1}D). \quad (4)$$

(d) If  $(M|D)$  is across a periodicity cell and  $X = \begin{pmatrix} x \\ x' \end{pmatrix}$  is the periodic dispersion vector (this is conventionally written as  $\begin{pmatrix} x_p \\ x'_p \end{pmatrix}$ ), but since in this paper we will deal

only with the dispersion vector and never with the free oscillation vector we can, without confusion, drop the subscript p), then

$$(M|D)X = MX+D = X$$

and

$$D = (1-M)X. \quad (5)$$

(e) For the  $\pi$ -straight section the optics-dispersion transfer matrix is  $(-1|0)$ .

### III. EFFECT OF $\pi$ -STRAIGHT SECTION INSERTION

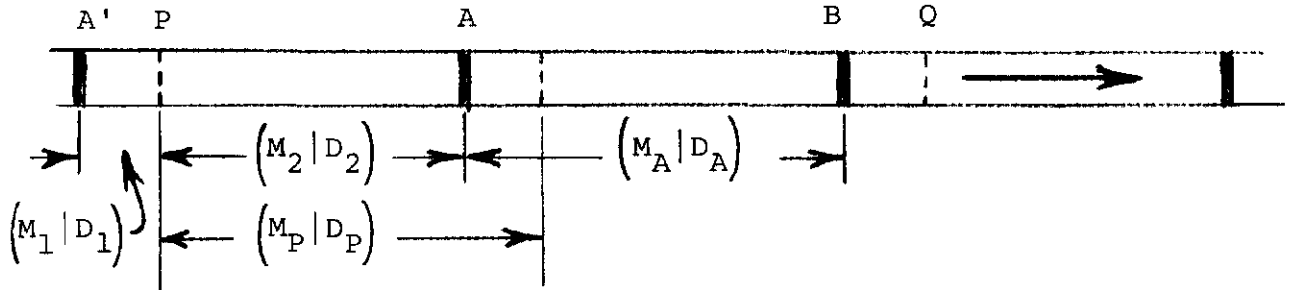


Figure 2

We start with a lattice without  $\pi$ -insertion (Figure 2). The distance between A and B is one repetition length which may contain many cells. We need the following relations between the optics-dispersion transfer matrices defined in Fig. 2. From A to B we have

$$(M_A|D_A) = (M_2|D_2) (M_1|D_1) = (M_2 M_1 | M_2 D_1 + D_2)$$

which gives

$$M_2 D_1 + D_2 = D_A = (1 - M_A) X_A. \quad (6)$$

From P to Q we have

$$\begin{aligned} (M_P | D_P)^2 &= (M_1 | D_1) (M_2 | D_2) (M_1 | D_1) (M_2 | D_2) \\ &= (M_1 M_2 M_1 M_2 | M_1 M_2 M_1 D_2 + M_1 M_2 D_1 + M_1 D_2 + D_1) \end{aligned}$$

which gives

$$M_1 M_2 M_1 D_2 + M_1 M_2 D_1 + M_1 D_2 + D_1 = (1 - M_P^2) X_P. \quad (7)$$

Now we insert  $\pi$ -straight sections at A, B, and all other homologous locations. The new transfer matrix from P to Q becomes

$$\begin{aligned} (M_1 | D_1) (-1 | 0) (M_2 | D_2) (M_1 | D_1) (-1 | 0) (M_2 | D_2) \\ = (M_1 M_2 M_1 M_2 | M_1 M_2 M_1 D_2 - M_1 M_2 D_1 - M_1 D_2 + D_1). \end{aligned}$$

Together with Eqs. (6) and (7) this gives for the new periodic dispersion vector at P,  $\bar{X}_P = \begin{pmatrix} \bar{x} \\ \bar{x}' \end{pmatrix}_P$ ,

$$\begin{aligned} (1 - M_P^2) \bar{X}_P &= M_1 M_2 M_1 D_2 - M_1 M_2 D_1 - M_1 D_2 + D_1 \\ &= M_1 M_2 M_1 D_2 + M_1 M_2 D_1 + M_1 D_2 + D_1 - 2M_1 (M_2 D_1 + D_2) \\ &= (1 - M_P^2) X_P - 2M_1 (1 - M_A) X_A \end{aligned} \quad (8)$$

whence, we get

$$\Delta X_P \equiv \bar{X}_P - X_P = -2 (1 - M_P^2)^{-1} M_1 (1 - M_A) X_A. \quad (9)$$

To simplify the right-hand-side expression we note first

$$\left(1-M_P^2\right)^{-1} = \frac{1-M_P^{-2}}{4\sin^2\mu}$$

where  $\mu$  is the phase advance across one repetition length (not including the  $\pi$ -insertion). Furthermore,

$$\begin{aligned}\left(1-M_P^{-2}\right)_{M_1} &= \left(1-M_2^{-1}M_1^{-1}M_2^{-1}M_1^{-1}\right)_{M_1} \\ &= M_1\left(1-M_1^{-1}M_2^{-1}M_1^{-1}M_2^{-1}\right) = M_1\left(1-M_A^{-2}\right)\end{aligned}$$

and

$$\begin{aligned}\left(1-M_A^{-2}\right)\left(1-M_A\right) &= \left(2-M_A-M_A^{-1}\right)\left(1+M_A^{-1}\right) \\ &= 2(1-\cos\mu)\left(M_A^{1/2}+M_A^{-1/2}\right)M_A^{-1/2} \\ &= 4\cos\frac{\mu}{2}(1-\cos\mu)M_A^{-1/2}\end{aligned}$$

where  $M_A^{-1/2}$  is the same as  $M_A$  except with the phase advance  $\mu$  replaced by  $-\frac{\mu}{2}$ . Altogether we have

$$\begin{aligned}\Delta X_P &= -2\left(1-M_P^2\right)^{-1}M_1\left(1-M_A\right)X_A \\ &= -\frac{1}{2\sin^2\mu}M_1\left(1-M_A^{-2}\right)\left(1-M_A\right)X_A \\ &= -\frac{1}{\cos\frac{\mu}{2}}M_1M_A^{-1/2}X_A.\end{aligned}\tag{10}$$

$M_1$  is the matrix from the beginning of the repetition length (point A' in Fig. 1) to P and by definition  $M_A^{-1/2}$  reduces the

phase advance in  $M_1$  by  $\frac{\mu}{2}$ . Therefore,  $M_1 M_A^{-1/2}$  has the form

$$M_1 M_A^{-1/2} = \begin{pmatrix} \sqrt{\frac{\beta_P}{\beta_A}} (\cos \phi_P + \alpha_A \sin \phi_P) & \sqrt{\beta_A \beta_P} \sin \phi_P \\ -\frac{1}{\sqrt{\beta_A \beta_P}} \left[ (\alpha_P - \alpha_A) \cos \phi_P + (1 + \alpha_A \alpha_P) \sin \phi_P \right] & \sqrt{\frac{\beta_A}{\beta_P}} (\cos \phi_P - \alpha_P \sin \phi_P) \end{pmatrix} \quad (11)$$

where

$$\phi_P = (\text{phase advance from } A' \text{ to } P) - \frac{\mu}{2}$$

and where all betatron oscillation functions  $\alpha_A$ ,  $\beta_A$ ,  $\alpha_P$ ,  $\beta_P$  and the phases are values before the insertion of the  $\pi$ -straight sections. Of course, Eq. (11) can be derived also by straight-forward computation. We are only interested in the first row  $\Delta x_P$  of the vector Eq. (10) and since P is the running variable point within the repetition length we can drop the subscript P. This gives

$$\Delta x = \bar{x} - x = -\frac{\sqrt{\beta}}{\cos \frac{\mu}{2}} \left[ (\cos \phi + \alpha_A \sin \phi) \sqrt{\frac{x_A}{\beta_A}} + \sin \phi \sqrt{\beta_A} x'_A \right] \quad (12)$$

with

$$\begin{aligned} \phi &= (\text{phase measured from beginning of repetition length}) - \frac{\mu}{2} \\ &= (\text{phase measured from "middle" of repetition length}). \end{aligned}$$

Eq. (12) can be derived in different ways, e.g., by matching the solutions of the orbit equations of the orbit equation with inversions at points A, B, etc. to form the closed orbit. The derivation given above seems to be the shortest and most lucid.

The new dispersion orbit-length increment per repetition length with the  $\pi$ -insertions is (The orbit-length increment in



the  $\pi$ -straight section is zero.)

$$\begin{aligned} \int_{-\mu/2}^{\mu/2} \frac{\bar{x}}{\rho} \beta d\phi &= \int_{-\mu/2}^{\mu/2} \frac{x}{\rho} \beta d\phi + \int_{-\mu/2}^{\mu/2} \frac{\Delta x}{\rho} \beta d\phi \\ &= \int_{-\mu/2}^{\mu/2} \frac{x}{\rho} \beta d\phi - \frac{1}{\cos \frac{\mu}{2}} \left[ (C + \alpha_A S) \frac{x_A}{\sqrt{\beta_A}} + S \sqrt{\beta_A} x'_A \right] \end{aligned} \quad (13)$$

where

$$\begin{cases} C \equiv \int_{-\mu/2}^{\mu/2} \frac{\beta^{3/2}}{\rho} \cos \phi d\phi \\ S \equiv \int_{-\mu/2}^{\mu/2} \frac{\beta^{3/2}}{\rho} \sin \phi d\phi \end{cases}$$

and  $\rho = \rho(\phi)$  is the radius of curvature of the on-momentum orbit. Now we see that because of the denominator  $\cos \frac{\mu}{2}$ , by judicious choice of  $\mu$  we can adjust the second term on the right-hand-side of Eq. (13) to cancel the first term to give zero dispersion orbit-length increment or infinite  $\gamma_t$ .

#### IV. CRUDE ESTIMATE AND EXAMPLES

To give a simple example let us assume that the  $\pi$ -straight sections are inserted at locations where  $\alpha_A = 0$ , hence  $x'_A = 0$ . The condition for zero dispersion orbit-length increment Eq. (13) then gives

$$\int_{-\mu/2}^{\mu/2} \frac{x}{\rho} \beta d\phi = \frac{C}{\cos \frac{\mu}{2}} \frac{x_A}{\sqrt{\beta_A}} \quad (14)$$

Now, for a very crude estimate we have

$$C = \int_{-\mu/2}^{\mu/2} \frac{\beta^{3/2}}{\rho} \cos \phi d\phi = \left\langle \frac{\beta^{3/2}}{\rho} \right\rangle \int_{-\mu/2}^{\mu/2} \cos \phi d\phi = 2 \left\langle \frac{\beta^{3/2}}{\rho} \right\rangle \sin \frac{\mu}{2} \quad (15)$$

where  $\langle \rangle$  denotes some kind of average value in the periodicity length from  $-\frac{\mu}{2}$  to  $\frac{\mu}{2}$ . Also

$$\int_{-\mu/2}^{\mu/2} \frac{x}{\rho} \beta d\phi = \left\langle \frac{\beta^{3/2}}{\rho} \right\rangle \left\langle \frac{x}{\sqrt{\beta}} \right\rangle \int_{-\mu/2}^{\mu/2} d\phi = \left\langle \frac{\beta^{3/2}}{\rho} \right\rangle \left\langle \frac{x}{\sqrt{\beta}} \right\rangle \mu \quad (16)$$

where  $\langle \rangle$  again denotes some kind of average. Assuming  $\left\langle \frac{\beta^{3/2}}{\rho} \right\rangle$  in Eq. (15) to be roughly equal to that in Eq. (16) and since  $\frac{x}{\sqrt{\beta}}$  is more or less constant in a normal lattice, hence  $\left\langle \frac{x}{\sqrt{\beta}} \right\rangle \approx \frac{x_A}{\sqrt{\beta_A}}$  we obtain by substituting Eqs. (15) and (16) in Eq. (14)

$$\frac{\mu}{2} \approx \tan \frac{\mu}{2}. \quad (17)$$

Let

$$\mu = (2n-1)\pi - 2\pi\epsilon \quad n = \text{integer.}$$

We have

$$\tan \frac{\mu}{2} = \cot \epsilon\pi$$

and

$$2\pi\nu = N(\mu+\pi) = 2\pi nN - 2\pi\epsilon N$$

or

$$\nu = nN - \epsilon N \quad (18)$$

where  $N$  is the number of symmetrically inserted  $\pi$ -straight sections and  $\nu$  is the betatron oscillation wave number including the  $\pi$ -insertions. In the first place  $\nu$  must have a value (integer)  $\pm \frac{1}{4}$ . Setting  $\epsilon N = \frac{1}{4}$  we get

$$\epsilon = \frac{1}{4N} \quad (19)$$

and that the integral part of  $\nu$  must be a multiple of  $N$ . Solving Eq. (18) for  $n$  in terms of  $\nu$  and inserting into  $\mu$  we get

$$\mu = 2\pi \left( \frac{\nu}{N} - \frac{1}{2} \right). \quad (20)$$

Substituting Eqs. (19) and (20) in Eq. (17) we get

$$\nu \approx N \left( \frac{1}{2} + \frac{1}{\pi} \cot \frac{\pi}{4N} \right). \quad (21)$$

This equation gives an approximate upper limit of  $\nu$  for a given number  $N$  of  $\pi$ -insertions. For low values of  $N$  we have

<u>N</u>	<u><math>\nu</math></u>	<u>N</u>	<u><math>\nu</math></u>
1	0.82	6	17.5
2	2.54	7	23.3
3	5.06	8	29.9
4	8.40	9	37.2
5	12.5	10	45.4

Suppose we use FODO cells similar to those of the NAL main ring and insert 6 ( $N = 6$ )  $\pi$ -straight sections to build up an infinite- $\gamma_t$  lattice for 400 BeV and  $\nu \approx 18 - \frac{1}{4}$  ( $n = 3$ ). There are 15 normal cells in between two  $\pi$ -insertions. At 400 BeV the orbit parameters obtained from computer runs using SYNCH are

orbit radius = 988.0 m

bending magnet field = 19.225 kG

quadrupole field gradient =  $\pm 213.0$  kG/m

$v_x = 17.772$

$v_y = 17.818$

$\gamma_t^2 = \begin{cases} -1811 & \text{mid-D insertion} \\ -4778 & \text{mid-F insertion} \end{cases}$

Other parameters are given in the SYNCH output attached. Instead of  $\gamma_t$  which may be imaginary we print out  $\gamma_t^2$ . The two values of  $\gamma_t^2$  correspond to the cases in which the  $\pi$ -straight sections are inserted in the middle of either the defocusing or the focusing quadrupoles. The large negative  $\gamma_t^2$  values (instead of  $\infty$ ) indicate that we have overshoot in reducing the dispersion orbit-length increment and the increment is actually slightly negative in both cases (negative momentum compaction). This is presumably because the  $v_x$  values chosen are closer to 18 than  $\frac{1}{4}$ .

The  $\beta$ -values are rather large in the  $\pi$ -straight sections which is inherent in the design of the  $\pi$ -straight section. A serious drawback of these lattices is the very large local maximum  $x$  ( $x_p$  or  $x_{eq}$ ) which makes very stringent demand on the magnet aperture at these locations. This is, of course, inherent in the method employed to compensate for the dispersion orbit-length increase. These large local maximum  $x$  can be reduced by increasing the number of  $\pi$ -insertions (say, from 6 to 9).

The modifications of SYNCH to print out  $\gamma_t^2$  was made by Dr. J. MacLachlan. His assistance is gratefully acknowledged.

**NORMAL CELL**

BETATRON FUNCTIONS THROUGH C

0	0.00000	0.00000	35.3505	-000	1.23260	.00105	5.94564	0.00000	102.8260	.000	0.00000	0.00000	13.0
1	1.05880	00	35.0276	-634	1.26306	.05615	6.00239	.00166	100.7878	1.713	0.00000	0.00000	13.0
2	3.17500	00	74.9932	-721	3.38143	.05615	6.23644	.00512	93.7434	1.630	0.00000	0.00000	13.6
3	9.24567	5	49.0846	-956	3.74877	.06487	7.00604	.01662	75.3782	1.394	0.00000	0.00000	6.6
4	9.55000	0	49.5722	-970	3.76854	.06497	7.00478	.01727	74.5319	1.382	0.00000	0.00000	6.6

5	15.62100	9	.05423	67.8877	-1.207	4.18885	.07360	7.93019	.03184	59.1917	1.146	0.00000	0.00000	7.6
6	15.92581	0	.05670	63.6272	-1.219	4.21128	.07360	7.97667	.03266	58.4967	1.134	0.00000	0.00000	7.5
7	21.99697	9	.06956	79.8659	-1.456	4.68457	.09233	8.93683	.05130	46.1534	.897	0.00000	0.00000	5.7
8	22.37127	0	.06917	80.7582	-1.468	4.70966	.08233	8.98556	.05236	45.6130	.885	0.00000	0.00000	5.7
9	28.37180	9	.07993	100.0221	-1.705	5.23593	.09105	10.90111	.07619	36.2975	.648	0.00000	0.00000	6.3

10	24.67630	0.0941	101.0653	-1.717	5.26368	-0.9105	10.75312	0.07753	35.9058	0.637	0.00000	0.00000	5.9	
11	29.74397	0F	0.0870	102.9081	-0.000	5.11289	0.0137	10.14437	0.08232	35.2507	0.000	0.00000	0.00000	5.9
12	30.81027	0F	0.0873	101.0653	1.0735	5.26595	-0.0894	13.75131	0.08711	35.97555	-0.636	0.00000	0.00000	5.9
13	32.91807	00	0.0817	93.9886	1.635	5.07845	-0.0894	9.59529	0.0811	38.7650	-0.719	0.00000	0.00000	6.2
14	34.98307	8	0.0864	75.5932	1.398	4.56504	-0.0821	9.59426	0.11837	48.9106	-0.956	0.00000	0.00000	6.9

15	39.29347	0	0.9929	74.7418	1.386	4.54059	-.08021	8.64534	-.11935	49.5169	0.00000	0.00000	7.0
16	45.35490	8	.11301	59.3576	1.149	4.08015	-.07148	7.73039	-.13673	62.7044	0.00000	0.00000	7.9
17	45.66927	0	.11454	58.6611	1.137	4.05936	-.07148	7.65905	-.13750	63.4423	0.00000	0.00000	7.9
18	51.71928	8	.1322	46.7013	.899	3.65990	-.06276	6.80448	-.15112	79.6455	0.00000	0.00000	8.9
19	52.70463	0	.13477	45.7563	.888	3.63177	-.06276	6.76434	-.15171	80.5346	0.00000	0.00000	8.9

20	58.11529	1503	36.4204	.550	3.27729	-.05403	6.03493	.16250	99.7483	-1.700	0.00000	0.00000	1.0
21	58.42007	0	15937	.638	3.26082	-.05403	6.03230	.16298	100.7485	-1.712	0.00000	0.00000	1.0
22	59.48680	90	16114	.000	3.23260	.00105	5.94564	.16465	102.6260	.000	0.00000	0.00000	1.1

THETA = .06981317 QX =  
GAMMA-Y SQUARE = 20.4271635E+01

	MAXIMA	BETAXI	I I I =	102.90832138	XEQI	I I I =	5.31289263	BETAYI	I I I =	102.62603720
--	--------	--------	---------	--------------	------	---------	------------	--------	---------	--------------

\*\*\* SUPERIORIOO CONSISTS OF C570 +JSC

MID-D INSERTION

RETATION FUNCTIONS THROUGH S																			
POS	S	PSIX	RETX	ALPHAX	KFO	DMFO	BTAX	PSIX	RETX	ALPHAY	VEY	OVED	DET						
0	0.00000	0.00000	35.3506	-0.000	-30970	-76391	5.94564	0.00000	102.6260	.000	0.00000	0.00000	15.1						
1	29.18136	0000	59.4426	-826	21.98382	-76391	7.70391	0.00000	113.9155	-284	0.00000	0.00000	15.5						
2	30.25016	00	60.1439	-172	22.59737	-38461	7.75525	0.00000	113.5630	-2.212	0.00000	0.00000	15.6						
3	31.31696	00	58.7167	1.158	22.80195	-00165	7.66268	0.00000	120.4710	-4.302	0.00000	0.00000	15.9						
4	32.38376	00	55.3640	2.059	22.53185	-38789	7.43397	0.00000	132.1435	-6.706	0.00000	0.00000	11.4						
5	33.45056	00	50.0345	2.813	21.97685	-76710	7.07351	0.00000	149.4313	-9.598	0.00000	0.00000	12.2						
6	37.71776	000	29.2714	2.053	18.70348	-76710	5.41031	0.00000	242.6932	-12.257	0.00000	0.00000	15.5						
7	38.78456	00	14.572	1.432	18.05243	-4.5532	5.05729	0.00000	264.8631	-8.399	0.00000	0.00000	15.2						
8	39.85136	00	15.273	23.068	17.72908	-15180	4.80487	0.00000	278.1003	-3.935	0.00000	0.00000	16.6						
9	40.91816	00	16.015	21.6217	17.72756	-14896	4.64991	0.00000	281.4503	.813	0.00000	0.00000	16.7						
10	41.98496	00	16.833	21.0741	18.04785	-45242	4.59065	0.00000	274.6736	5.502	0.00000	0.00000	16.5						
11	71.16811	0000	58.6982	-1.338	41.25098	-45242	7.65821	0.00000	50.5097	2.179	0.00000	0.00000	7.1						
12	102.35167	0000	37.039	-2.726	44.45410	-45242	13.31366	0.00000	20.2563	-1.143	0.00000	0.00000	4.5						
13	101.41847	00	37.134	179.4506	44.53302	-30469	13.41121	0.00000	23.2233	-1.656	0.00000	0.00000	4.8						
14	102.48527	00	176.0005	3.299	43.80597	-1.05629	13.26652	0.00000	27.4074	-2.289	0.00000	0.00000	5.2						
15	103.55207	00	165.9514	5.064	42.28611	-1.78978	12.98221	0.00000	33.1119	-3.090	0.00000	0.00000	5.7						
16	104.61887	00	150.4376	8.391	40.00396	-2.48888	12.26530	0.00000	40.7536	-4.116	0.00000	0.00000	6.3						
17	106.88607	000	47.4695	6.365	29.38039	-2.48888	9.35251	0.00000	83.9007	-5.995	0.00000	0.00000	3.1						
18	108.95287	00	39.237	75.821	26.98383	-2.01378	8.70388	0.00000	95.5243	-4.835	0.00000	0.00000	7.7						
19	111.01967	00	34.474	67.6849	25.07723	-1.56317	8.22709	0.00000	104.2832	-3.326	0.00000	0.00000	11.2						
20	112.08647	00	38.737	62.3417	23.62579	-1.15605	7.89569	0.00000	109.5462	-1.578	0.00000	0.00000	17.4						
21	113.15327	00	39.016	59.4826	22.60323	-76391	7.70391	0.00000	110.9341	.285	0.00000	0.00000	15.5						
22	142.33622	0000	50.000	35.3506	30.970	-76391	5.94564	0.00000	102.6261	.000	0.00000	0.00000	13.1						
23	201.82382	C	66.414	35.3506	-21.47005	-3297	5.94564	0.00000	102.6260	.000	0.00000	0.00000	13.1						
24	261.31022	C	82.828	35.3506	-19.22367	-43518	5.94564	0.00000	102.6260	.000	0.00000	0.00000	13.1						
25	320.79702	C	94.242	35.3506	4.86398	-76391	5.94564	0.00000	102.6261	.000	0.00000	0.00000	13.1						
26	380.28182	C	1.15655	35.3506	27.36492	-35999	5.94564	0.00000	102.6260	.000	0.00000	0.00000	13.1						
27	439.77062	C	1.32069	35.3506	26.33444	-40332	5.94564	0.00000	102.6260	.000	0.00000	0.00000	13.1						
28	499.25792	C	1.48443	35.3506	2.89643	-76391	5.94564	0.00000	102.6260	.000	0.00000	0.00000	13.1						
29	558.74422	C	1.64897	35.3506	-20.27461	-38601	5.94564	0.00000	102.6260	.000	0.00000	0.00000	13.1						
30	618.23102	C	1.81311	35.3506	-20.58223	-37275	5.94564	0.00000	102.6260	.000	0.00000	0.00000	13.1						
31	677.71782	C	1.97725	35.3506	2.27278	-76391	5.94564	0.00000	102.6260	.000	0.00000	0.00000	13.1						
32	737.20462	C	2.14138	35.3506	26.06132	-41934	5.94564	0.00000	102.6260	.000	0.00000	0.00000	13.1						
33	796.69142	C	2.30552	35.3506	27.64633	-33814	5.94564	0.00000	102.6260	.000	0.00000	0.00000	13.1						
34	856.17622	C	2.46966	35.3506	5.48622	-76572	5.94564	0.00000	102.6260	.000	0.00000	0.00000	13.1						
35	915.66502	C	2.63340	35.3506	-18.86580	-44753	5.94564	0.00000	102.6260	.000	0.00000	0.00000	13.1						
36	975.15182	C	2.79794	35.3506	-21.72462	-30595	5.94564	0.00000	102.6260	.000	0.00000	0.00000	13.1						
37	1034.63862	C	2.96208	35.3506	-30370	-76391	5.94564	0.00000	102.6260	.000	0.00000	0.00000	13.1						

THEIA 3 5.2813522 0X = 17.77246329 OF = 17.81819445  
GAMMA-T SQUARE = -18.110907E+02  
MAXIMA RETAX 131= 179.86062717 REO( 131)= 44.51301928 RETAY( 91= 281.45094544

MAXIMA	REYAX(	1)= 102.37832139	XFO4	1)= 5.31289263	REFTAYC	11)= 102.62603727
--------	--------	------------------	------	----------------	---------	-------------------

7730 MULFELS

	***	CSTR	CYC	22	//	0000	QF	QF	QF	000	00	07	0D
	*	.	.	.	//	0F	QF	QE	QF	000	00	07	0D
					//	0F	QF	QE	QF	000	00	07	0D

SUPERSEDED CONSISTS OF 579 +150

MID-F INSERTION

POS	S	PSIX	RETAX	ALPHAX	XFO	DXEO	SETAX	PSIV	RETAI	ALPHAY	YEC	DYEO	SET
0	0.07000	0.07000	102.9083	-0.000	-9.91806	4.3129	10.14437	0.00000	35.2307	-0.000	0.00000	0.00000	5.9
1	29.14336	0.000	111.1843	-2.284	11.66841	4.3129	10.14437	0.00000	59.4317	-0.828	0.00000	0.00000	7.7
2	30.25016	0.000	109.7900	1.583	12.02153	4.2973	10.47877	0.00000	62.3761	-1.911	0.00000	0.00000	7.2
3	31.31636	0.000	104.5118	3.335	12.15709	4.2402	10.22310	0.00000	67.6537	-3.132	0.00000	0.00000	5.2
4	32.39375	0.000	95.7303	4.847	12.37262	-1.0213	9.78418	0.00000	75.8347	-4.583	0.00000	0.00000	5.7
5	33.45795	0.000	84.0791	6.010	11.75966	-3.8498	9.16941	0.00000	87.4457	-6.367	0.00000	0.00000	3.3
6	37.71776	0.000	40.8284	4.126	10.12686	-3.8498	6.39971	0.00000	150.4347	-6.324	0.00000	0.00000	12.2
7	38.78456	0.000	33.1686	3.098	9.80683	-2.1593	5.75922	0.00000	165.9558	-6.067	0.00000	0.00000	12.8
8	39.85136	0.000	27.4530	2.295	9.66482	-0.5073	5.23927	0.00000	176.0126	-3.303	0.00000	0.00000	13.2
9	40.91816	0.000	23.2554	1.660	9.69826	-1.1352	4.82238	0.00000	179.8903	-3.301	0.00000	0.00000	13.4
10	41.98495	0.000	20.2789	1.147	9.30775	-2.7982	4.50321	0.00000	177.2801	-2.723	0.00000	0.00000	13.3
11	71.15931	0.000	50.5675	-2.184	18.07334	-2.7982	7.11109	0.00000	58.7849	1.338	0.00000	0.00000	7.5
12	100.35167	0.000	275.2799	-5.516	26.24012	-2.7982	16.59156	0.00000	21.1123	-0.048	0.00000	0.00000	4.5
13	101.41847	0.000	282.3757	-8.816	26.30029	-1.6720	16.79511	0.00000	21.6544	-0.464	0.00000	0.00000	4.6
14	132.48527	0.000	278.7211	3.942	25.88447	-6.1119	16.69494	0.00000	23.1148	-0.914	0.00000	0.00000	4.6
15	103.55207	0.000	265.4577	4.416	25.00719	-1.04412	16.29287	0.00000	25.5999	-1.430	0.00000	0.00000	5.0
16	104.61847	0.000	243.2413	12.283	23.66345	-1.45816	15.59619	0.00000	29.2911	-2.951	0.00000	0.00000	5.4
17	108.84607	0.000	149.7796	9.619	17.44118	-1.45816	12.23945	0.00000	50.0304	-2.839	0.00000	0.00000	7.0
18	139.85287	0.000	132.4539	6.720	16.03922	-1.17416	11.50986	0.00000	55.2519	-2.056	0.00000	0.00000	7.4
19	111.01967	0.000	120.7569	4.311	14.92841	-3.1148	10.98894	0.00000	58.6964	-1.154	0.00000	0.00000	7.6
20	112.08647	0.000	113.4353	2.216	14.08960	-6.6535	10.66936	0.00000	60.1158	-1.169	0.00000	0.00000	7.7
21	113.15327	0.000	111.1803	-2.284	13.50454	-4.3129	10.54447	0.00000	59.4078	-0.828	0.00000	0.00000	7.7
22	142.27662	0.000	102.9083	0.000	9.91806	-4.3129	10.14437	0.00000	35.2307	-0.000	0.00000	0.00000	5.9
23	201.82342	0.000	102.9083	0.000	-35.11858	-1.8439	10.14437	0.00000	35.2307	-0.000	0.00000	0.00000	5.9
24	251.31022	0.000	102.9083	0.000	-31.83113	-2.4289	10.14437	0.00000	35.2307	-0.000	0.00000	0.00000	5.9
25	320.79702	0.000	102.9083	0.000	7.58321	4.3497	10.14437	0.00000	35.2307	-0.000	0.00000	0.00000	5.9
26	330.27382	0.000	102.9083	0.000	44.78980	2.0503	10.14437	0.00000	35.2307	-0.000	0.00000	0.00000	5.9
27	339.77062	0.000	102.9083	0.000	43.60721	-2.2328	10.14437	0.00000	35.2307	-0.000	0.00000	0.00000	5.9
28	399.25742	0.000	102.9083	0.000	5.17225	-4.3339	10.14437	0.00000	35.2307	-0.000	0.00000	0.00000	5.9
29	558.74422	0.000	102.9083	0.000	-33.11891	-2.2094	10.14437	0.00000	35.2307	-0.000	0.00000	0.00000	5.9
30	612.23102	0.000	102.9083	0.000	-34.07078	2.0744	10.14437	0.00000	35.2307	-0.000	0.00000	0.00000	5.9
31	677.71782	0.000	102.9083	0.000	3.32354	4.3510	10.14437	0.00000	35.2307	-0.000	0.00000	0.00000	5.9
32	737.27462	0.000	102.9083	0.000	42.61274	2.4061	10.14437	0.00000	35.2307	-0.000	0.00000	0.00000	5.9
33	796.69122	0.000	102.9083	0.000	5.62160	-1.8686	10.14437	0.00000	35.2307	-0.000	0.00000	0.00000	5.9
34	856.17822	0.000	102.9083	0.000	5.42772	-4.3155	10.14437	0.00000	35.2307	-0.000	0.00000	0.00000	5.9
35	915.66502	0.000	102.9083	0.000	-30.77030	-2.5547	10.14437	0.00000	35.2307	-0.000	0.00000	0.00000	5.9
36	975.15182	0.000	102.9083	0.000	-35.87331	-1.7012	10.14437	0.00000	35.2307	-0.000	0.00000	0.00000	5.9
37	1034.63862	0.000	102.9083	0.000	-31.806	4.3129	10.14437	0.00000	35.2307	-0.000	0.00000	0.00000	5.9

THETA = 6.29314522 CX = 17.77246330 CY = 17.61819444

GAMMA-Y SQUARE = -47.781238E+02

MAXIMA RETAXI 131= 292.07573930 XEOI 331= 45.62359546 RETAYI 91= 179.88027938